Thermodynamic and kinetic study on interfacial reaction and diamond graphitization of Cu–Fe-based diamond composite*

Li Wen-Sheng(李文生)[a)†], Zhang Jie(张 杰)[a)], Dong Hong-Feng(董洪锋)[a)], Chu Ke(褚 克)[a)], Wang Shun-Cai(王顺才)[b)], Liu Yi(刘 毅)[a)], and Li Ya-Ming(李亚明)[a)]

[a)] *State Key Laboratory of Advanced Non-Ferrous Materials, Lanzhou University of Technology, Lanzhou* 730050, *China*
[b)] *National Centre for Advanced Tribology, Engineering Sciences, University of Southampton, Southampton, SO17 1BJ, UK*

(Received 11 May 2012; revised manuscript received 18 June 2012)

Cu–Fe based diamond composites used for saw-blade segments are directly fabricated by vacuum and pressure-assisted sintering. The carbide forming elements Cr and Ti are added to improve interfacial bonding between diamond and the Cu–Fe matrix. The interfacial reactions between diamond/graphite and Cr or Ti, and diamond graphitization are investigated by thermodynamics/kinetics analyses and experimental methods. The results show that interfacial reactions and graphitization of diamond can automatically proceed thermodynamically. The Cr_3C_2, Cr_7C_3, $Cr_{23}C_6$, and TiC are formed at the interfaces of composites by reactions between diamond and Cr or Ti; diamond graphitization does not occur because of the kinetic difficulty at 1093 K under the pressure of 13 MPa.

Keywords: thermodynamics, kinetics, diamond composites, diamond graphitization

PACS: 81.05.uj **DOI:** 10.1088/1674-1056/22/1/018102

1. Introduction

Diamond composite tools are widely used for sawing, cutting, grinding, and trimming stone, concrete and tiles. These tool materials consist of three main components: diamond grain, binder phase, and the interface between the diamond surface and the metallic binder. The performances of each component are vital to the comprehensive performance of the tool. Diamond acting as the cutting element is one of the allotropic forms of carbon,[1] and is renowned for its outstanding physical, chemical, and mechanical properties.[2,3] The binder phases should have approximately the same coefficient of thermal expansion and thermal conductivity as those of diamond in order to improve the matching performance between diamond and matrix. Cu–Fe based diamond composite is a kind of metal matrix composite (MMC),[4] in which the interfacial transient layer can distinctly enhance interfacial bonding strength and determine the overall properties of the composite, because the interfacial phase is usually formed between diamond and the metallic binder during composite fabrication processing.[5]

Usually, metals do not provide satisfactory junctions to diamond because diamond has chemical inertness and most metals in their molten fluid state cannot wet diamond adequately. From many previous wettability studies, appreciable wetting of diamond by melted metals occurs only in these cases where interfacial reactions between the metal and diamond take place.[6] Obviously, good wetting characteristics in a bond system cause the matrix to be excellently held on to the diamond. On the other hand, diamond is a metastable allotrope of carbon at ambient temperature and pressure so that diamond particles may be graphitized especially if there are catalytic metals in the matrix, deteriorating the final cutting performance. Thus, it is of great significance to examine the graphitization tendency of diamond particles in the high temperature sintering process of Cu–Fe based composite.[7] All these disadvantages restrict the applications of diamond tools. Consequently, adequate interfacial reaction but not graphitization is a fundamental requirement for enhancing the performance of diamond composite tools.[8] To solve these interface problems, using different alloys containing active elements capable of establishing chemical interactions with diamond has been proven to significantly improve the interfacial bonding of a Cu based diamond composite. It has been reported that good interfacial bonding but not graphitization is achieved in diamond reinforced Cu–Cr or Cu–Si matrix composite.[9,10] Unfortunately, there was no previous research on how these active elements play a role thermodynamically and kinetically. Therefore, it is very necessary to investigate the mechanism of these active elements in thermodynamics and kinetics.

This paper is devoted to the study of interfacial reactions and diamond graphitization by thermodynamics/kinetics analyses and experimental research, aiming to improve the performances of Cu–Fe based diamond composites.

*Project supported by the National Natural Science Foundation of China (Grant No. 51165021) and the Science Fund for Distinguished Young Scholars of Gansu Province, China (Grant No. 111RJDA0103).

†Corresponding author. E-mail: wensheng-li@sohu.com

© 2013 Chinese Physical Society and IOP Publishing Ltd

2. Experimental detail

2.1. Specimen preparation

Table 1 shows the compositions of Cu–Fe based diamond composite. The metallic and diamond powders were blended by a three-dimensional vortex mixer (TD-2) for 1 h. The powder mixture was placed into a cylindrical graphite die and sintered in a vacuum and pressure-assisted sintering machine (RYJ-2000Z) at 1093 K and 13 MPa with a holding time of 3 min. After the synthesis process, the disc-shaped samples were obtained after getting rid of the graphite felt left on the surface of the composites.

Table 1. Compositions of Cu–Fe based diamond composite.

Ingredient	wt.%
Cu	45–55
Fe	35–45
Co–Cr pre-alloyed powder	5–8
Cr	1–3
Ti	1–3
Diamond	2

2.2. Structure and graphitization analyses

Phase analysis was carried out using X-ray diffraction (XRD) (Rigaku D/Max-2400) technique with a copper target (Cu–Kα radiation, $\lambda = 1.54$ Å). Raman scattering analysis was tested on a laser Raman spectrometer (in Via–Reflex) with a 0.15 cm^{-1} resolution to identify the graphitization tendency of diamond. Scanning electron microscopy (SEM) (6700F) with an energy dispersive X-ray (EDX) spectrum was employed to detect the distribution of elements in the interface zone near diamond.

3. Theoretical calculation

3.1. Theory of standard reaction heat effect

In the synthesis process of Cu–Fe based diamond composite, some interfacial carbides such as Cr_7C_3, Cr_3C_2, $Cr_{23}C_6$, and TiC would be formed between diamond and strong carbide forming elements in specific thermodynamic conditions.[11] The Gibbs free energy change of each of these carbides forming reactions is calculated by the theory of standard reaction heat effect method

$$a\mathrm{A} + b\mathrm{B} \rightarrow c\mathrm{C} + d\mathrm{D}. \tag{1}$$

In the Gibbs–Helmholtz equation,[12]

$$\mathrm{d}\left(\frac{\Delta G_T^\theta}{T}\right) = -\frac{\Delta H_T^\theta}{T^2}\mathrm{d}T, \tag{2}$$

and the Kirchhoff equation

$$\mathrm{d}\Delta H_T^\theta = \Delta C_P \mathrm{d}T, \tag{3}$$

where ΔG_T^θ as a function of the atmospheric temperature T denotes the change in Gibbs free energy, ΔH_T^θ denotes the change in enthalpy, and ΔC_P denotes the change in constant pressure specific heat capacity. Here, the superscript θ means the standard state. The ΔG_T^θ is calculated according to the following expressions:

$$\begin{aligned}\Delta G_T^\theta &= -\Delta A_1 T\ln T - \frac{1}{2}\Delta A_2\times 10^{-3}T^2 \\ &\quad - \frac{1}{2}\Delta A_3\times 10^5 T^{-1} - \frac{1}{6}\Delta A_4\times 10^{-6}T^3 \\ &\quad + A_5' T + A_5, \end{aligned}\tag{4}$$

$$\begin{aligned}C_P &= A_1 + A_2\times 10^{-3}T + A_3\times 10^5 T^{-2} \\ &\quad + A_4\times 10^{-6}T^2, \end{aligned}\tag{5}$$

$$\Delta C_P = (cC_{P,\mathrm{C}} + dC_{P,\mathrm{D}}) - (aC_{P,\mathrm{A}} - bC_{P,\mathrm{B}}), \tag{6}$$

$$\begin{aligned}A_5 &= \Delta H_{298}^\theta - \Delta A_1 298 - \frac{1}{2}\Delta A_2\times 10^{-3}\times 298^2 \\ &\quad + \Delta A_3\times 10^5\times 298^{-1} \\ &\quad - \frac{1}{3}\Delta A_4\times 10^{-6}\times 298^3, \end{aligned}\tag{7}$$

$$\begin{aligned}A_5' &= \frac{\Delta G_{298}^\theta}{298} + \Delta A_1\ln 298 + \frac{1}{2}\Delta A_2\times 10^{-3}\times 298 \\ &\quad + \frac{1}{2}\Delta A_3\times 10^5\times 298^{-2} \\ &\quad + \frac{1}{6}\Delta A_4\times 10^{-6}\times 298^2 - 298^{-1}A_5, \end{aligned}\tag{8}$$

$$\Delta G_{298}^\theta = \Delta H_{298}^\theta - 298\Delta S_{298}^\theta, \tag{9}$$

$$\begin{aligned}\Delta H_{298}^\theta &= \left(cH_{298,\mathrm{C}}^\theta + dH_{298,\mathrm{D}}^\theta\right) \\ &\quad - \left(aH_{298,\mathrm{A}}^\theta + bH_{298,\mathrm{B}}^\theta\right), \end{aligned}\tag{10}$$

$$\begin{aligned}\Delta S_{298}^\theta &= \left(cS_{298,\mathrm{C}}^\theta + dS_{298,\mathrm{D}}^\theta\right) \\ &\quad - \left(aS_{298,\mathrm{A}}^\theta + bS_{298,\mathrm{B}}^\theta\right), \end{aligned}\tag{11}$$

where A_1, A_2, A_3, and A_4 are fitting parameters of C_P; A_5 and A_5' are the integration constants of the Kirchhoff equation and Gibbs–Helmholtz equation; $H_{298,\mathrm{A}}^\theta$, $S_{298,\mathrm{B}}^\theta$, and $C_{P,\mathrm{C}}$ are the enthalpy value of material A, the entropy value of material B, and the constant pressure specific heat of material C, respectively. These thermodynamic parameters can be found in Ref. [13].

3.2. Theory of classical thermodynamics

In calculating the change of Gibbs free energy in diamond graphitization, the theory of classical thermodynamics[12] is introduced as follows:

$$\Delta G_T^P = \Delta G_T^\theta + \int_0^P \Delta V \mathrm{d}P, \tag{12}$$

$$\Delta G_T^\theta = \Delta H_T^\theta - T\Delta S_T^\theta, \tag{13}$$

$$\Delta H_T^\theta = \Delta H_{298}^\theta + \int_{298}^T \Delta C_P \mathrm{d}T, \tag{14}$$

$$\Delta S_T^\theta = \Delta S_{298}^\theta + \int_{298}^T \Delta C_P \mathrm{d}(\ln T), \tag{15}$$

where ΔG_T^P as a function of T and P denotes the Gibbs free energy change in diamond graphitization. Consequently, ΔG_T^P

is calculated under thermodynamic conditions (T, P) as

$$\begin{aligned}\Delta G_T^P &= \left(\Delta H_{298}^\theta - T\Delta S_{298}^\theta\right) \\ &+ \left(\int_{298}^{T} \Delta C_P \mathrm{d}T - T\int_{298}^{T} \Delta C_P \mathrm{d}\ln T\right) \\ &+ \int_0^P \Delta V \mathrm{d}P. \end{aligned} \tag{16}$$

The ΔV is calculated as follows:[13–15]

$$\begin{aligned}\Delta V &= 1.820 + 1.596\times10^{-4}T - 4.339\times10^{-8}T^2 \\ &+ 1.403\times10^{-11}T^3 - 6.320\times10^{-16}T^4 \\ &- 1.385\times10^{-19}T^5 - 0.089P + 6.083\times10^{-3}P^2 \\ &+ 3.063\times10^{-4}P^3 + 8.420\times10^{-6}P^4 \\ &- 9.240\times10^{-8}P^5. \end{aligned} \tag{17}$$

3.3. Gibbs free energy change of interfacial reactions between diamond/graphite and Cr or Ti

The calculation results of Gibbs free energy change in interfacial reactions between diamond/graphite and Cr or Ti at 298–1200 K and standard atmospheric pressure are presented as follows:

$$3\mathrm{Cr} + 2\mathrm{C}_{(\mathrm{d})} \rightarrow \mathrm{Cr_3C_2},$$

$$\begin{aligned}\Delta \mathrm{G}_T^\theta &= -54.259T\ln T + 0.036T^2 + 872400T^{-1} \\ &- 0.0000045T^3 + 343.133T \\ &- 109441.483, \end{aligned} \tag{18}$$

$$3\mathrm{Cr} + 2\mathrm{C}_{(\mathrm{g})} \rightarrow \mathrm{Cr_3C_2},$$

$$\begin{aligned}\Delta \mathrm{G}_T^\theta &= -72.333T\ln T + 0.062T^2 + 1345000T^{-1} \\ &- 0.00001T^3 + 744.180T \\ &- 110762.634, \end{aligned} \tag{19}$$

$$7\mathrm{Cr} + 3\mathrm{C}_{(\mathrm{d})} \rightarrow \mathrm{Cr_7C_3},$$

$$\begin{aligned}\Delta \mathrm{G}_T^\theta &= -86.953T\ln T + 0.0697T^2 + 1062000T^{-1} \\ &- 0.000011T^3 + 527.220T \\ &- 202926.634, \end{aligned} \tag{20}$$

$$7\mathrm{Cr} + 3\mathrm{C}_{(\mathrm{g})} \rightarrow \mathrm{Cr_7C_3},$$

$$\begin{aligned}\Delta \mathrm{G}_T^\theta &= -114.064T\ln T + 0.108T^2 + 1772000T^{-1} \\ &- 0.0000192T^3 + 706.278T \\ &- 218451.845, \end{aligned} \tag{21}$$

$$\mathrm{Ti} + \mathrm{C}_{(\mathrm{d})} \rightarrow \mathrm{TiC},$$

$$\begin{aligned}\Delta \mathrm{G}_T^\theta &= -18.703T\ln T + 0.01125T^2 + 429800T^{-1} \\ &- 0.0000003T^3 + 132.206T \\ &- 193448.582, \end{aligned} \tag{22}$$

$$\mathrm{Ti} + \mathrm{C}_{(\mathrm{g})} \rightarrow \mathrm{TiC},$$

$$\begin{aligned}\Delta \mathrm{G}_T^\theta &= -27.75T\ln T + 0.0241T^2 + 665300T^{-1} \\ &- 0.0000003T^3 + 191.888T \\ &- 194857.227, \end{aligned} \tag{23}$$

$$23\mathrm{Cr} + 6\mathrm{C}_{(\mathrm{d})} \rightarrow \mathrm{Cr_{23}C_6},$$

$$\begin{aligned}\Delta \mathrm{G}_T^\theta &= -245.59T\ln T + 0.2145T^2 + 3761000T^{-1} \\ &- 0.00003463T^3 + 1516.241T \\ &- 488734.25, \end{aligned} \tag{24}$$

$$23\mathrm{Cr} + 6\mathrm{C}_{(\mathrm{g})} \rightarrow \mathrm{Cr_{23}C_6},$$

$$\begin{aligned}\Delta \mathrm{G}_T^\theta &= -299.82T\ln T + 0.2916T^2 + 5179400T^{-1} \\ &- 0.00005199T^3 + 1874.352T \\ &- 497186.11, \end{aligned} \tag{25}$$

where $\mathrm{C}_{(\mathrm{d})}$ and $\mathrm{C}_{(\mathrm{g})}$ are referred to as diamond and graphite, respectively.

Figure 1 shows ΔG_T^θ in carbide formation as a function of atmospheric temperature T calculated through Eqs. (18)–(25), predicting the possibility of carbonization of Cr and Ti at a certain temperature. It shows that ΔG_T^θ values of these reactions are all negative and the tendency of reactions is $\mathrm{Cr_{23}C_6}$ > $\mathrm{Cr_7C_3}$ > TiC > $\mathrm{Cr_3C_2}$ at the same temperature. It can also be clearly seen that ΔG_T^θ values of chrome carbide reactions decline with the increase of temperature, but ΔG_T^θ value of titanium carbide reaction increases with the increase of temperature. For $\mathrm{Cr_{23}C_6}$ and TiC, the tendencies of reactions between diamond and Cr, Ti are larger than those of reactions between graphite and Cr, Ti at 298–1200 K. For $\mathrm{Cr_3C_2}$ and $\mathrm{Cr_7C_3}$, the tendency of diamond-Cr is slightly lower than that of graphite–Cr at temperatures lower than approximately 500 K, whereas the reaction tendency is opposite above 500 K.

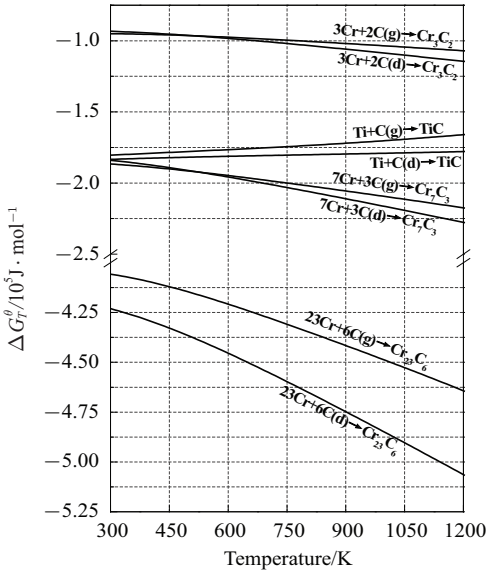


Fig. 1. Gibbs free energy changes of interfacial carbide reactions between diamond/graphite and Cr or Ti.

3.4. Gibbs free energy change in diamond graphitization

The calculation results of ΔG_T^P of diamond graphitization from 298 K to 1200 K are as follows:

$$\begin{aligned}\Delta G_T^P &= \left(\Delta H_{298}^\theta - T\Delta S_{298}^\theta\right) \\ &\quad + \left(\int_{298}^{T} \Delta C_p \mathrm{d}T - T\int_{298}^{T} \Delta C_p \mathrm{d}\ln T\right) + \int_0^P \Delta V \mathrm{d}P \\ &= 1409.052 - 59.688T - 0.013T^2 + 2.893\times 10^{-6}T^3 \\ &\quad - 2.364\times 10^5 T^{-1} + 9.207T\ln T + 1820P \\ &\quad - 0.160TP - 4.339\times 10^{-5}T^2P \\ &\quad + 1.403\times 10^{-8}T^3P - 6.320\times 10^{-13}T^4P \\ &\quad - 1.385\times 10^{-16}T^5P - 44.5P^2 + 2.028P^3 - 0.076P^4 \\ &\quad + 1.684\times 10^{-3}P^5 - 1.540\times 10^{-5}P^6, \end{aligned} \tag{26}$$

where P is in units of GPa.

Figure 2 shows the values of ΔG_T^P in diamond graphitization as a function of atmospheric temperature T and pressure P according to Eq. (26). As seen, the values of ΔG_T^P of diamond graphitization is negative in a temperature range of 298–1200 K and a pressure range of 0.01–0.1 GPa. The values of ΔG_T^P decreases as temperature rises but increases as pressure increases. Under this specific experimental condition, the value of ΔG_T^P of graphitization is –5392 J/mol at 1093 K and 0.013 GPa, showing that it is a much larger value than that of interfacial reactions.

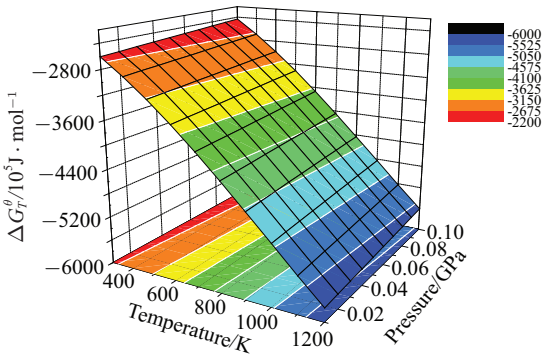


Fig. 2. (color online) Gibbs free energy of graphitization of diamond.

4. Experimental results

Figure 3 is Raman scattering spectrum of embedded diamond grains in the breaking section of the sintered specimen. As seen, a sharp first-order scattering peak from diamond at the position of 1332 cm^{-1} is detected and the graphite peak at the position of 1581 cm^{-1} is not detected in Fig. 3, indicating that diamond in the sample sintered at 1093 K and 13 MPa is not graphitized in the sintering process.

Figure 4 shows XRD patterns of the sample sintered at 1093 K and 13 MPa. Besides Cu and Fe matrix phases, Cr_7C_3, $Cr_{23}C_6$, Cr_3C_2, and TiC are also identified under such thermodynamic conditions, even though these carbide forming elements are negligible as predicted by the present thermodynamic calculation analysis. It is also found that diamond peaks are detected, but no graphite peak is detected.

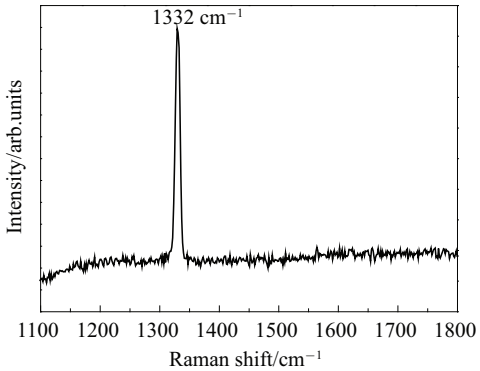


Fig. 3. Raman scattering spectrum of diamond in the segment sintered at 1093 K and 13 MPa.

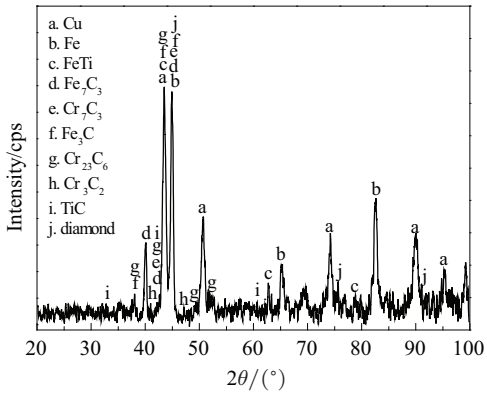


Fig. 4. XRD pattern of Cu–Fe based sample sintered at 1093 K and 13 MPa.

Figure 5 is the results of EDX line analysis of element distribution in the interface zone near diamond. As seen, Cr and Ti are enriched in the interface zone and carbon atoms diffuse into the interface-matrix area. The interface layer is more than 7 μm as shown by the weight fraction of carbon, chromium and titanium in Fig. 5.

5. Discussion

5.1. Interfacial carbide reaction

In terms of thermodynamics, ΔG_T^θ values of Cr_7C_3, Cr_3C_2, $Cr_{23}C_6$, and TiC formed at 1093 K by reactions between diamond and Cr or Ti are –222.154, –111.609, –495.874, and –178.494 J/mol, respectively. The values of ΔG_T^θ of those carbides formed by reactions between graphite and Cr or Ti are –213.488, –105.302, –456.627, and –168.182 J/mol, respectively. The values of ΔG_T^θ of carbides formed by reactions between diamond

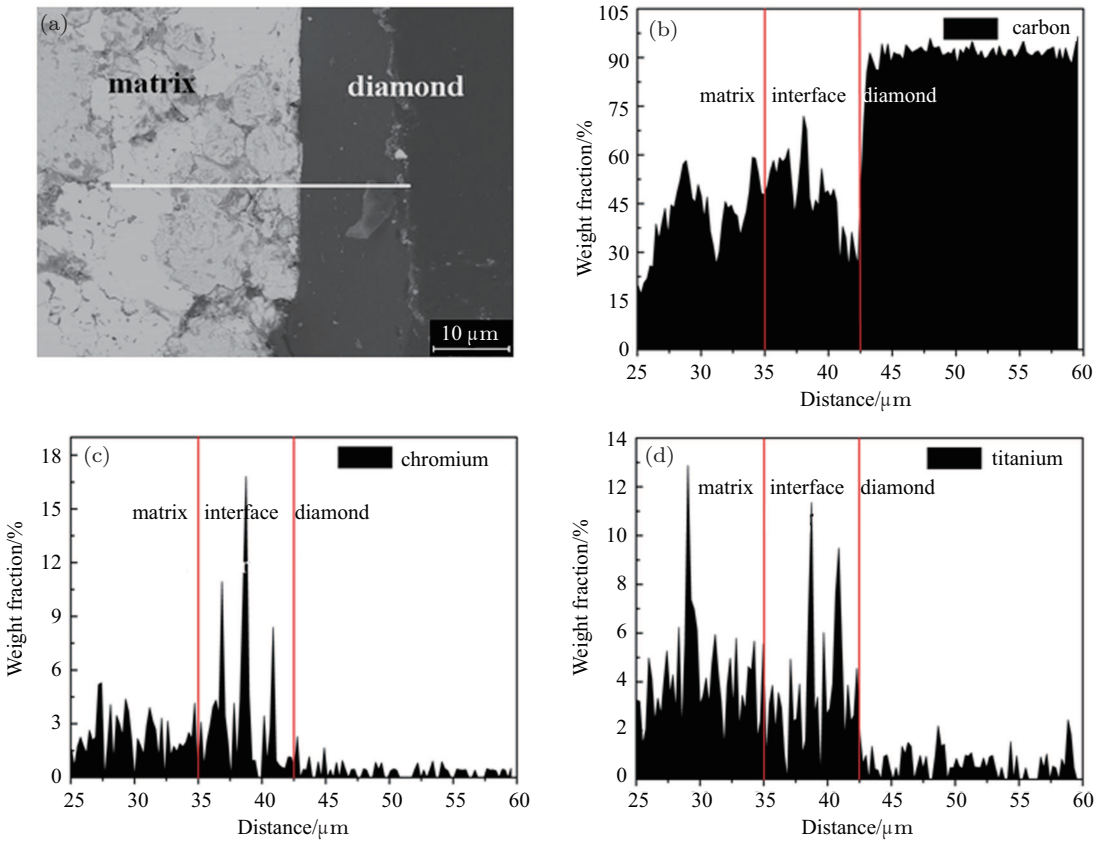


Fig. 5. (color online) EDX line analysis of the distribution of elements in the interface zone near diamond. (a) The breaking section SEM image of the sintered specimen; (b) EDX line analysis of carbon weight distribution; (c) EDX line analysis of chromium weight distribution; (d) EDX line analysis of titanium weight distribution.

and Cr or Ti are lower than those between graphite and Cr or Ti, indicating that the process of transforming Cr and Ti into carbides is automatic at 1093 K, and the diamond–Cr/Ti reaction is more likely than the graphite–Cr/Ti reaction. The thermodynamic analysis predicts the direction of reaction, but the energy levels of transition state and consequently the amount of activation energy in the reaction processes have not been estimated well so far. Hence, the reaction rate of the process cannot be predicted by the analysis described above.

In terms of kinetics, the formation of Cr_7C_3, Cr_3C_2, $Cr_{23}C_6$, and TiC carbide phases reduces the concentrations of Cr and Ti atoms in the interface zone near diamond, resulting in different concentrations of Cr and Ti atoms between the interface zone and matrix. The variations of Cr concentration and Ti concentration cause atom concentration gradients which provide the driving force of transporting these atoms from the matrix into the interface zone. On the other hand, the exothermic reactions[16] provide the required reaction energy for forming these carbides. The higher the reaction temperature, the faster the reaction process will be. In the experimental sintering process, diamond offers carbon atoms to form the carbide nuclei at the surface dislocation of diamond. Owing to the high concentration of carbon atoms near the diamond, $Cr_3C_2$and TiC nucleate close to the diamond and grow up to the side of the matrix alloy. The carbon atoms further diffuse from the surface of diamond into the matrix alloy to form Cr_3C_2, TiC, Cr_7C_3, and $Cr_{23}C_6$ which constitute the interfacial reaction layer. At the same time, Cr and Ti atoms in the matrix continue diffusing into diamond and lead to high Cr concentration and Ti concentration in the reaction layer close to diamond as seen in Fig. 5.

Figure 6 illustrates the details of the formation mechanism of the interfacial microstructure and phase. The formation of the reaction layer of the matrix alloy is due to the diffusion of carbon atoms on the surface of the diamond into the matrix alloy to form carbides comprised of Cr_3C_2, TiC,

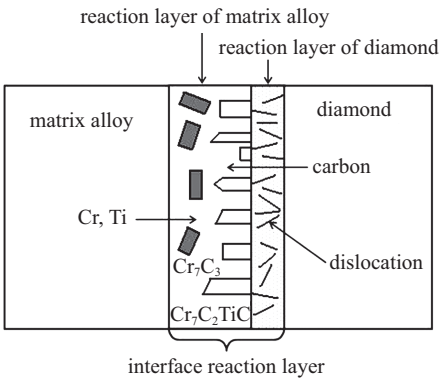


Fig. 6. Schematic of the diamond and matrix interface forming mechanism model.

Cr_7C_3, and $Cr_{23}C_6$, which is identified by XRD patterns in Fig. 4. The Cr_3C_2 and TiC prefer to nucleate near diamond and grow up to the formation of a matrix alloy, owing to the high concentration of carbon atoms close to diamond. The Cr_7C_3 and $Cr_{23}C_6$ are formed in the zone where the concentration of carbon atoms is low. The reaction layer of the diamond is formed by reactions between Cr, Ti, and carbon atoms on the surface of the diamond.

5.2. Graphitization of diamond

Raman spectra analysis shown in Fig. 3 indicates that graphitization does not occur at 1093 K and 13 MPa. According to thermodynamic calculation, the values of ΔG_T^P of diamond graphitization under the experimental condition of 1093 K and 13 MPa is negative and diamond graphitization could occur. However, the Gibbs free energy variation is just the necessary condition of phase transformation.

From the viewpoint of kinetics, diamond and graphite have different carbon lattice arrangements, and diamond is a metastable allotrope of carbon even at low temperature. The thermodynamic and kinetic relationship of transition between diamond and graphite is shown in Fig. 7. Graphite rather than diamond is the thermodynamically preferred (minimum energy) state, but the activation energy values needed for conversion from diamond to graphite are 730 kJ/mol on (110) plane and 1060 kJ/mol on (111) plane[17] so at experimental temperature (1093 K) and pressure (13 MPa), this conversion is extremely slow. This conversion process starts to be noticeable at around 1273 K.

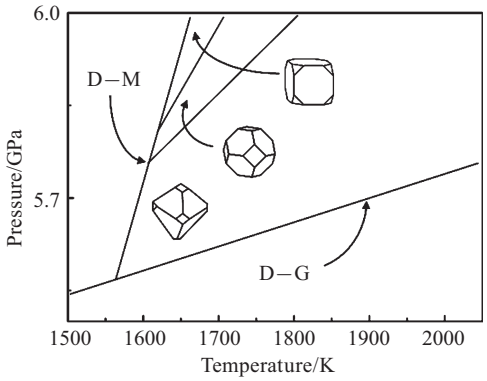


Fig. 7. Phase diagram for carbon.[18]

Actually, diamond graphitization is related to sintering temperature, sintering atmosphere, the purity of diamond, and so on. At the sintering temperature of 1093 K, the structure of diamond remains stable due to kinetic difficulty in rebuilding the lattice.[15] As temperature increases, the kinetic difficulty of diamond turning into graphite decreases.[19] If diamond reacts with oxygen in the atmosphere, CO or CO_2 is produced, leading to small pits formed on the surface of diamond particles. These small pits make the specific surface of diamond particles increase, resulting in an acceleration of graphitization.[7] Fe and Ni ingredients of the matrix of the diamond composite and the contact of the diamond surface by Fe and Ni can play a catalytic role in reducing the activation energy of graphitization. These factors could lead to diamond graphitization, but the low temperature, vacuum atmosphere, fast sintering and interfacial reactions can reduce the corrosion of the diamond surface, increase the starting temperature of graphitization and difficulty of lattice arrangements and, in turn, suppress the diamond graphitization.

The probability of phase transition from diamond to graphite (f_g) is

$$f_g = \exp\left[-\left(E_a - \Delta' G_T^P\right)/RT\right], \tag{27}$$

where $\Delta' G_T^P$ is Gibbs free energy of diamond minus that of graphite (i.e., $\Delta' G_T^P = -\Delta G_T^P$), E_a is the activation energy of phase transition, R is the gas constant ($R = 8.31$ J/mol · K), and f_g is 10^{-8} at 1093 K and 13 MPa, and may be ignored.

6. Conclusions

(1) The Gibbs free energy changes of Cr_7C_3, Cr_3C_2, $Cr_{23}C_6$, and TiC by reactions between diamond and Cr, Ti, and diamond graphitization are negative at the conditions of 1093 K and 13 MPa. The reaction of carbides Cr_3C_2, TiC, Cr_7C_3,and $Cr_{23}C_6$ carbides and the diamond graphitization can automatically proceed in thermodynamics.

(2) Interfacial reactions and interfacial diffusion can occur under the conditions of 1093 K and 13 MPa. The these reactions generated heat, concentration gradient, and dislocation on the surface of diamond offer the energy, diffusion driving force, and nucleation cores, which are required by the reactions in kinetics.

(3) Diamond graphitization does not occur under the condition of 1093 K and 13 MPa. The diamond graphitization can be suppressed by low temperature, vacuum atmosphere, fast sintering and interfacial reactions.

References

[1] Field J E 1992 *The Properties of Natural and Synthetic Diamond* (London: Elsevier Academic Press)
[2] Zhou L, Jia X P, Ma H A, Zheng Y J and Li Y T 2008 *Chin. Phys.* B **17** 4665
[3] Zhou L, Jia X P, Ma H A, Zheng Y J and Li Y T 2009 *Chin. Phys.* B **18** 333
[4] Li W S, Zhang J, Wang S C, Dong H F, Li Y M and Liu Y 2012 *Rare Metals* **31** 81
[5] Chu K, Jia C, Liang X and Chen H 2010 *Rare Metals* **29** 86
[6] Chu K, Jia C, Liang X and Chen H 2010 *Int. J. Miner. Metall. Mater.* **17** 234
[7] Shao W Z, Ivanov V V, Zhen L, Cui Y S and Wang Y 2003 *Mater. Lett.* **58** 146
[8] Hsieh Y Z, Chen J F and Lin S T 2000 *J. Mater. Sci.* **35** 5383
[9] Chu K, Liu Z F, Jia C C, Chen H, Liang X B, Gao W J, Tian W H and Guo H 2010 *J. Alloys Compd.* **490** 453
[10] Moriguchi H, Tsuduki K, Ikegauya A, Miyamoto Y and Morisada Y 2007 *Int. J. Refract. Met. Hard Mater.* **25** 237
[11] Wang C Y, Zhou Y M, Zhang F L and Xu Z C 2009 *J. Alloys Compd.* **476** 884
[12] Mortimer R G 2008 *Physical Chemistry* (3rd edn.) (London: Elsevier Academic Press) p. 179

[13] Ye D L and Hu J H 2002 *Practical Thermodynamic Data Handbook of Inorganic Substances* (Beijing: Metallurgy Industry Press) (in Chinese)
[14] Li L 2008 *Valence Electron Theory and Thermodynamics Analysis of Diamond Growth Mechanism at HPHT* (PhD. dissertation) (Jinan: Shandong University) (in Chinese)
[15] Sung J 2000 *J. Mater. Sci.* **35** 6041
[16] Kollman P 1993 *Chem. Rev.* **93** 2395
[17] Tanaka H, Shimada S, Ikawa N and Yoshinaga M 2001 *Key Eng. Mater.* **196** 69
[18] Qin J M, Zhang Y, Cao J M and Tian L F 2011 *Acta Phys. Sin.* **60** 058102 (in Chinese)
[19] Oliveira L, Bobrovnitchii G S and Filgueira M 2007 *Int. J. Refract. Met. Hard Mater.* **25** 328